Electroencephalography and clinical Neurophysiology, 1987, 66: 75–81
Elsevier Scientific Publishers Ireland, Ltd.

EEG 01764

Technical Section

Mapping of scalp potentials by surface spline interpolation

F. Perrin, J. Pernier, O. Bertrand, M.H. Giard and J.F. Echallier

U280 – INSERM, 151 Cours Albert Thomas, 69003 Lyon (France)

(Accepted for publication: 24 March, 1986)

Summary Evoked potentials and EEGs record punctate electrical activity at electrode sites. To represent the overall potential distribution on the entire scalp it is necessary to interpolate between these sampled values. Surface splines are mathematical tools for interpolating functions of two variables.

In comparison to the classical methods of interpolation, based on linear combination of the potentials of the 4 nearest electrodes, spline methods are smoother, give more precisely located extrema and converge faster toward the 'true' potential surface when the number of recording electrodes is increased. These advantages are at the expense of lengthier computation time.

Key words: interpolation; spline

The difficulty of interpreting potential data recorded from scalp electrodes, when presented as multiple raw curves, has led to the use of scalp potential distribution mapping. These maps transform apparently complex wave forms into rather simple surface distributions and indicate readily the sites of maximal scalp activity (Duffy et al. 1979; Buchsbaum et al. 1982; Thickbroom et al. 1984). For practical reasons only a small number (between 12 and 24 in commercial systems, up to 48 in research laboratories) of recording electrodes are commonly used. This introduces the issue of how to make the best out of this small number of data, i.e., which interpolation method to use? Of course in no case can the interpolation technique compensate for an inadequate spatial sampling.

In this paper we wish to discuss the interpolation method. Among the methods which have been used to interpolate scalp potential data, some restrict the coordinates of the electrodes to be located in a rectangular mesh (Ueno and Matsuoka 1976; Lehmann et al. 1978; Ragot and Rémond 1978; Darcey et al. 1980; Duff 1980; Denoth et al. 1983) while others are able to deal with electrodes irregularly disposed on the scalp (Duff 1980; Coppola et al. 1982; Wood and Wolpaw 1982; Sandini et al. 1983; Ashida et al. 1984; Thickbroom et al. 1984).

The classically used interpolation method is the 4-nearest neighbours (4-NN) method (Shepard 1968). It presents some advantages: ease of computation and arbitrary location of the recording electrodes, and some disadvantages: map discontinuities and extrema always located at electrode sites.

We shall present another method: the surface spline interpolation, which allows interpolation of data recorded from irregularly disposed electrodes, gives a continuous surface and better estimates the locations of the extrema, these advantages being at the expense of a lengthier computation time.

A surface spline is the surface obtained by minimizing the bending energy of an infinite plate constrained to pass through known points. This method has been used for interpolating wing deflections in aerospace calculations (Harder and Desmarais 1972).

To test the performance of an interpolation method one needs to know the potential distribution everywhere on the scalp. Since in practice this is not feasible we have chosen to simulate the real

evoked potential by using a spherical volume conductor with a current dipole inside it. In this way we have compared the spline method with the 4-NN method.

Methods

(1) mth degree surface splines

Let n be the number of electrodes, $e_i = (x_i, y_i)$ the coordinates of the ith electrode in the projection plane, and z_i the value of the electric potential at electrode e_i. One may show (Duchon 1976) that for m equals 2, the mth degree surface spline $U_m(x, y)$ which interpolates the potential values z_i at e_i is:

$$U_m(x, y) = \sum_{i=1}^{n} p_i k_{m-1}(x - x_i, y - y_i) + q_{m-1}(x, y),$$

where $q_{m-1}(x, y)$ is an $(m-1)^{th}$ degree polynomial in 2 variables:

$$q_{m-1}(x, y) = \sum_{d=0}^{m-1} \sum_{k=0}^{d} q_{kd} x^{d-k} y^k,$$

and where k_{m-1} is given by:

$$k_{m-1}(s, t) = (s^2 + t^2)^{m-1} \log(s^2 + t^2).$$

This function U_m depends on the $n + m(m+1)/2$ coefficients p_i and q_{ij}.

Let Q denote the vector of the q_{ij}'s, P the vector of the p_i's and Z the vector of the z_i's:

$$Q = (q_{00}, q_{01}, q_{11}, \ldots, q_{m-1\,m-1})',$$

$$p = (p_1, p_2, \ldots, p_n)',$$

$$z = (z_1, z_2, \ldots, z_n)'.$$

Then Q and P are solutions of the following matrix equations (Duchon 1976):

$$K \cdot P + E \cdot Q = Z,$$

$$E' \cdot P = 0,$$

where the matrices K and E are:

$$K = (k_{ij}) = k_{m-1}(x_i - x_j, y_i - y_j),$$

$$E = \begin{pmatrix} 1 & x_1 & y_1 & x_1^2 & x_1 y_1 & \ldots & x_1 y_1^{m-2} & y_1^{m-1} \\ \vdots & \vdots & \vdots & & & & & \vdots \\ 1 & x_n & y_n & x_n^2 & x_n y_n & \ldots & x_n y_n^{m-2} & y_n^{m-1} \end{pmatrix}$$

It should be noted first that the smoothness of these interpolates increases with m. In fact the first $(m-1)$ derivatives of U_m are continuous. Secondly, when the number of electrodes increases, the error between the interpolated surface $U_m(x, y)$ and the true potential value decreases and the speed of convergence is known. If h denotes the greatest distance which exists between a point $e = (x, y)$ of the region of the scalp which is to be represented and its nearest electrode then the root mean square error decreases as h^{m-1} when h decreases (i.e., when the number of electrodes increases; Duchon 1978).

We shall consider only 3 surface splines, corresponding to m equals 2, 3 and 4, which will be referred to in the following as methods (1), (2) and (3).

(2) k-nearest neighbours methods

Let $e = (x, y)$ denote the coordinates of an arbitrary point on the scalp, $e_i = (x_i, y_i)$, with $i = 1, \ldots, k$, its k-nearest neighbours and d_i ($d_i^2 = (x - x_i)^2 + (y - y_i)^2$) the distance between e and e_i. The k-nearest neighbours interpolation formulae are of the following type:

$$V_m(x, y) = \left(\sum_{i=1}^{k} z_i d_i^m \right) \Big/ \left(\sum_{i=1}^{k} d_i^m \right).$$

From the formula it follows that extrema are always located at some e_i. If k is strictly less than the number of electrodes, then V_m is not continuous and one may show that the root mean square error as well as the maximum absolute error decrease as h when the number of electrodes increases.

We shall consider only 4-NN methods, and among these, the 3 corresponding to m equals -1, -2 or -3, which will be referred to in the following as methods (-1), (-2) and (-3).

(3) Method for error evaluation

In order to compare interpolated potential values with known potential distributions, we have chosen to use the 3-concentric-shell head model (Ary et al. 1981) consisting of a homogeneous

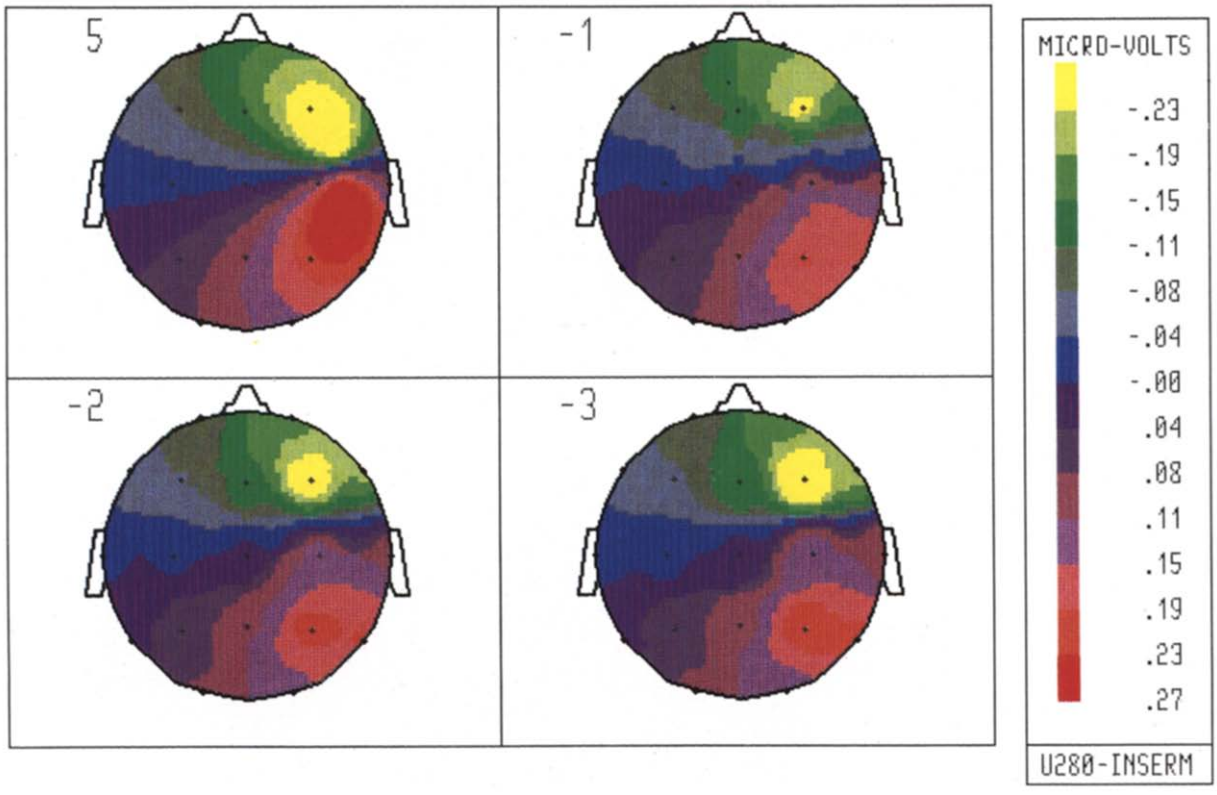

Fig. 1. Maps interpolated from 19 data points generated by a tangential dipole ($\theta = 60°$, $\varphi = 20°$, eccentricity = 0.8) with the 4-NN methods (−1), (−2) and (−3). Top left map (5) shows the 'true' potential distribution.

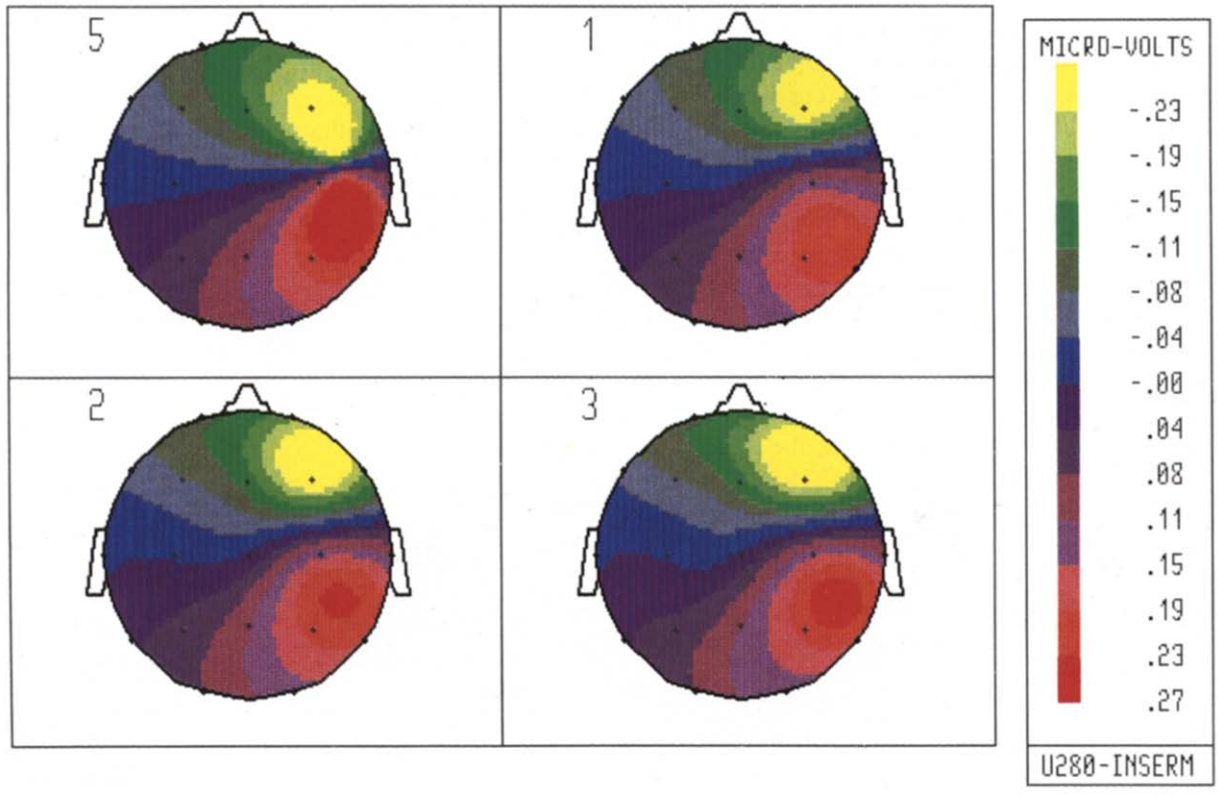

Fig. 2. Maps interpolated from 19 data points generated by a tangential dipole ($\theta = 60°$, $\varphi = 20°$, eccentricity = 0.8) with the surface spline methods (1), (2) and (3). Top left map (5) shows the 'true' potential distribution.

TABLE I

θ, φ: usual spherical coordinates; θ: azimuth with respect to C_z; φ: longitude with respect to T_4.

	θ (°)	φ (°)	θ (°)	φ (°)
C_z	0	0	30	45
C_4	45	0	–	135
F_z	–	90	–	225
C_3	–	180	–	315
P_z	–	270	66.5	75
F_4	61.8	49.3	–	105
F_3	–	130.7	–	255
P_3	–	229.3	–	285
P_4	–	310.7	69.5	20
T_4	90	0	–	160
F_8	–	36	–	200
Fp_2	–	72	–	340
Fp_1	–	108	90	18
F_7	–	144	–	54
T_3	–	180	–	90
T_5	–	216	–	126
O_1	–	252	–	162
O_2	–	288	–	198
T_6	–	324	–	234
			–	240
			–	306
			–	342

sphere of neural tissue (conductivity σ, radius r_1) surrounded by two concentric spherical shells representing respectively the skull (conductivity σ_s, radius r_2) and the scalp (conductivity σ, radius R) with $r_1/R = 0.87$, $r_2/R = 0.92$ and $\sigma_s/\sigma = 0.0125$.

For each current dipole the 'true' values as well as the interpolated values were computed for each method at 5783 points regularly distributed on a hemisphere. From these values maximum errors, root mean square errors and extrema localization errors were calculated. This was done for 65 dipoles having different eccentricities and orientations. To compare the errors, the moment of each dipole was adjusted to generate at the surface of the sphere a maximum potential value of 1.

Two sets of electrode locations were used: a set of 19 electrodes located as in the international 10-20 system and a denser set of 41 regularly disposed electrodes which included the first set of 19 electrodes. The left part of Table I gives the coordinates of the first set, and the right part gives the coordinates of the additional second set.

Results and Discussion

Comparing the 4-NN methods (−1), (−2) and (−3) it appeared that method (−2) was systematically better than either method (−1) or (−3). This appears visually in Fig. 1 and numerically in Table II where the means, over all 65 different dipoles, of the ratio of RMS errors of the different methods are given.

In the case of the spline methods (1), (2), (3) a similar conclusion in favour of method (2) was obtained (Fig. 2 and Table II).

For the 4-NN method (−2) and the spline method (2), Fig. 3 shows the dependence of the RMS errors on the eccentricity of the dipole and on the number of electrodes. Figs. 4 and 5 illustrate the same relationships for maximum errors and extrema localization errors. These figures show the value of method (2), at least for dipoles of eccentricities up to 0.6 when 19 electrodes are used and in all cases for 41 electrodes.

In these 3 figures one may note that, on the logarithmic scale, the distance between the two spline lines is at least twice the distance between the two 4-NN lines. This is in accordance with the predicted rates of convergence of the errors which are proportional to, at least, h^2 for spline method (2) and to h for the 4-NN method (−2).

Walter et al. (1984) have already proposed, on aesthetic grounds, that either method (−3) or (−2) should be preferred to method (−1). This can also be seen in Fig. 1. In the same figure one sees clearly that the extrema necessarily occur at an electrode location, whereas this is not the case for the spline methods (Fig. 2). The smoothness

TABLE II

Results obtained with maps interpolated from 19 potential data.

4-NN methods	Spline methods
Mean of $\frac{\text{RMSE method (−1)}}{\text{RMSE method (−2)}}$	Mean of $\frac{\text{RMSE method (1)}}{\text{RMSE method (2)}}$
1.18 ± 0.11	1.69 ± 1.38
Mean of $\frac{\text{RMSE method (−3)}}{\text{RMSE method (−2)}}$	Mean of $\frac{\text{RMSE method (3)}}{\text{RMSE method (2)}}$
1.09 ± 0.11	1.49 ± 1.48

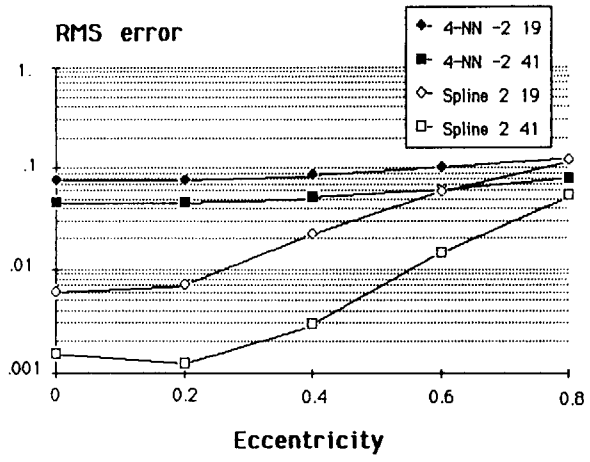

Fig. 3. RMS errors as function of the eccentricity of the dipoles. But for those of eccentricity 0, each point corresponds to the mean value of the RMS error of 15 different dipoles. The coefficients of variation of the 4-NN points increase, with the eccentricity, from 0.13 to 0.44, whereas those of the spline points decrease from 0.67 to 0.34.

properties of the spline interpolates also appear clearly in this last figure.

Figs. 3, 4 and 5 give an indication of the number of electrodes which must be used in order to obtain an error less than a predetermined value.

In comparing Figs. 1 and 2 with Fig. 6 it can be seen that 19 electrodes are barely sufficient to represent the spatial frequencies of this shallow

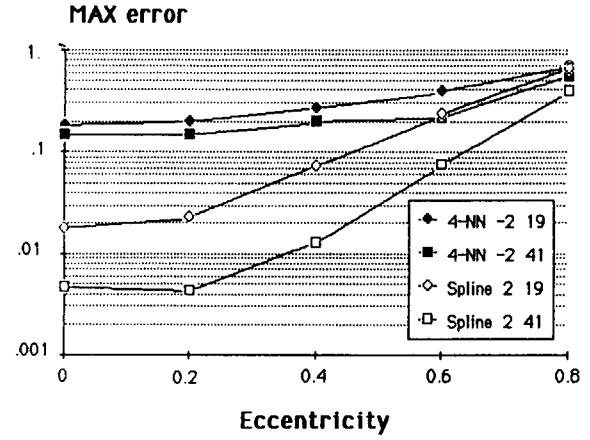

Fig. 4. Maximum errors as function of the eccentricity of the dipoles. The coefficients of variation of the 4-NN points increase, with the eccentricity, from 0.15 to 0.37, whereas those of the spline points decrease from 0.70 to 0.33.

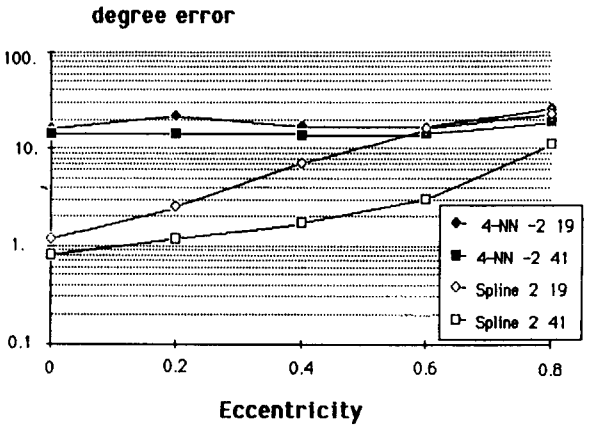

Fig. 5. Errors of localization of the extrema (in degrees) as function of the eccentricity of the dipoles. The coefficients of variation of the 4-NN points are of the order of 0.65, whereas those of the spline points decrease, when the eccentricity increases, from 1.7 to 0.6.

tangential dipole. Although this has been done with a simple head model one should recall Gevins (1984) who observed, in the case of visual evoked potentials, that above a spatial frequency of 0.1 c/cm the spectral amplitude decreases at a rate of 6 dB/octave. A spatial frequency of 0.1 c/cm corresponds to a distance peak-trough of 5 cm. In the case of a spherical head of 8 cm of radius and with 19 electrodes, the distance between electrodes is about 6.3 cm, whereas with 41 electrodes the distance is about 4.2 cm.

An illustration of how these interpolation methods represent experimental data is shown in Fig. 7 where the same somatosensory evoked potential data were interpolated either by method (-2) or method (2). One may note first that the maximum of the bottom map is not located at an electrode site and secondly that the gradient of the negative potential anterior to the zero middle line is much steeper with method (2) than with method (-2). If one were to interpret these maps in terms of a current dipole, method (2) would indicate a dipole more tangential and shallower than method (-2).

In conclusion, the spline interpolation method allows interpolation of potential data at irregularly located electrodes. The extrema of the interpolant are not necessarily located at electrode sites and are generally more precisely estimated than

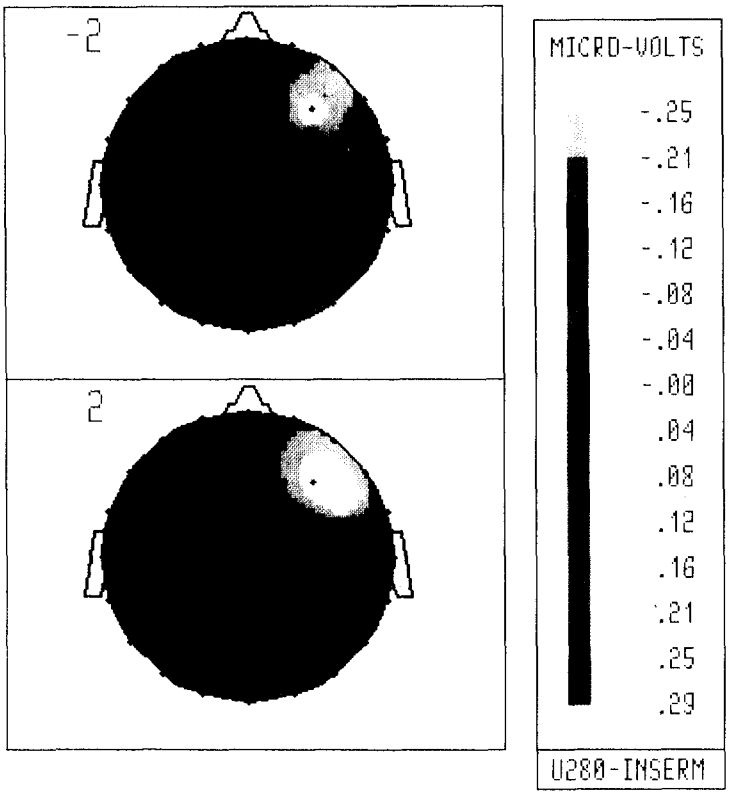

Fig. 6. Maps interpolated from 41 data points generated by a tangential dipole ($\theta = 60°$, $\varphi = 20°$, eccentricity = 0.8) with either (top) 4-NN method (-2) or (bottom) spline method (2).

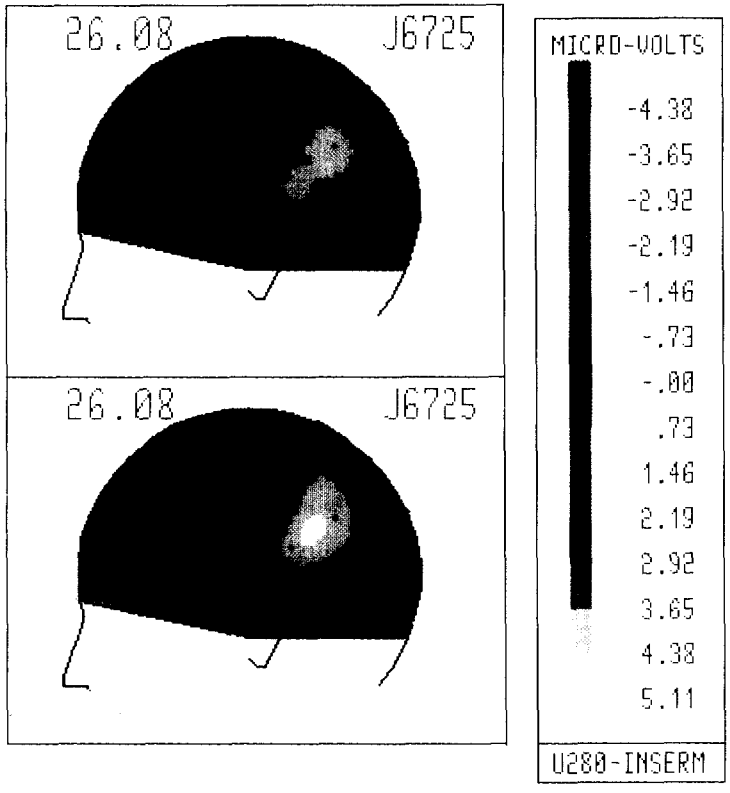

Fig. 7. Maps interpolated from 16 evoked potential data recorded 26 msec after a somatosensory stimulation of the right median nerve, with either (top) 4-NN method (-2) or (bottom) spline method (2). Reference electrode: left ear lobe.

with the 4-NN method. The surface splines are differentiable and their rates of convergence toward the 'true' potential surface are known and much faster than for the 4-NN method.

Résumé

Cartographie des potentiels de scalp par interpolation des surfaces de spline

Les potentiels évoqués comme l'électroencéphalographie n'enregistrent l'activité électrique du scalp qu'en des points précis correspondant à l'emplacement des électrodes. Pour avoir une représentation globale de la distribution du potentiel sur le scalp, il est nécessaire d'interpoler entre ces points de mesure. Les surfaces splines permettent d'effectuer de telles interpolations bi-dimensionnelles.

Par comparaison avec la méthode d'interpolation couramment utilisée basée sur la combinaison linéaire des potentiels des 4 plus proches électrodes la méthode des splines donne des surfaces plus régulières, les extrêmes sont mieux localisés et quand on augmente le nombre d'électrodes, les surfaces obtenues convergent plus rapidement vers la 'vraie' surface. En contrepartie le calcul de ces fonctions est plus long.

References

Ary, J.P., Klein, S.A. and Fender, D.H. Location of sources of evoked scalp potentials: corrections for skull and scalp thicknesses. IEEE Trans. bio-med. Engng, 1981, 28: 447–452.

Ashida, H., Tatsuno, J., Okamota, J. and Maru, E. Field mapping of EEG by unbiased polynomial interpolation. Comput. biomed. Res., 1984, 17: 267–276.

Brody, D.A., Terry, F.H. and Ideker, R.E. Eccentric dipole in a spherical medium: generalized expression for surface potentials. IEEE Trans. bio-med. Engng, 1973, 20: 141–142.

Buchsbaum, M.S., Rigal, F., Coppola, R., Cappelletti, J., King, C. and Johnson, J. A new system for gray-level surface distribution maps of electrical activity. Electroenceph. clin. Neurophysiol., 1982, 53: 237–242.

Coppola, R., Buchsbaum, M.S. and Rigal, F. Computer generation of surface distribution maps of measures of brain activity. Comput. Biol. Med., 1982, 12: 191–199.

Darcey, T.M., Ary, J.P. and Fender, D.H. Spatiotemporal visually evoked scalp potentials in response to partial-field patterned stimulation. Electroenceph. clin. Neurophysiol., 1980, 50: 348–355.

Denoth, F., Rappoli, R., Bruni, I., Navona, C. and Nencioni, C. Equipotential line map representation and temporal evolution of multichannel surface recorded CNV activity. In: Seventh Int. Conf. on Event Related Potentials of the Brain. Epic VII. Preliminary poster reports published by Università degli Studi di Firenze and Consiglio Nazionale delle Ricerche, Florence, September, 1983: 4–10.

Duchon, J. Interpolation des fonctions de deux variables suivant le principe de la flexion des plaques minces. R.A.I.R.O. Anal. num., 1976, 10: 5–12.

Duchon, J. Sur l'erreur d'interpolation des fonctions de plusieurs variables par les Dm splines. R.A.I.R.O. Anal. num., 1978, 12: 325–334.

Duff, T.A. Topography of scalp recorded potentials evoked by stimulation of the digits. Electroenceph. clin. Neurophysiol., 1980, 49: 452–460.

Duffy, F.H., Burchfield, J.L. and Lombroso, C.T. Brain electrical activity mapping (BEAM). A method for extending the clinical utility of EEG and evoked potential data. Ann. Neurol., 1979, 4: 309–321.

Gevins, A.S. Analysis of electromagnetic signals of the human brain: milestones, obstacles and goals. IEEE Trans. biomed. Engng, 1984, 31: 833–850.

Harder, R.L. and Desmarais, R.N. Interpolation using surface splines. J. Aircraft, 1972, 9: 189–191.

Lehmann, D. and Skrandies, W. Multichannel mapping of spatial distribution of scalp potential field evoked by checkerboard reversal to different retinal areas. In: D. Lehmann and E. Callaway (Eds.), Human Evoked Potentials. Applications and Problems. Plenum Press, New York, 1978: 201–214.

Ragot, R.A. and Rémond, A. EEG field mapping. Electroenceph. clin. Neurophysiol., 1978, 45: 417–421.

Sandini, G., Romano, P., Scotto, A. and Traverso, G. Topography of brain electrical activity: a bioengineering approach. Med. Prog. Tech., 1983, 10: 5–19.

Shepard, D.A. A two dimensional interpolation function for irregular-spaced data. Proc. ACM Nat. Conf., 1968: 517–524.

Thickbroom, G.W., Mastaglia, F.L. and Carroll, W.M. Spatiotemporal mapping of evoked cerebral activity. Electroenceph. clin. Neurophysiol., 1984, 59: 425–431.

Ueno, S. and Matsuoka, S. Topographic computer display of abnormal E.E.G. activities in patients with brain lesions. Digest of papers of the 11th International Conference on Medical and Biological Engineering. Medical Engineering Section, National Research Council, Ottawa, 1976: 216–219.

Walter, D.O., Etevenon, P., Pidoux, B., Tortrat, D. and Guillou, S. Computerized topo-EEG spectral maps: difficulties and perspectives. Neuropsychobiology, 1984, 11: 264–272.

Wood, C.C. and Wolpaw, J.R. Scalp distribution of human auditory evoked potentials. Evidence for overlapping sources and involvement of auditory cortex. Electroenceph. clin. Neurophysiol., 1982, 54: 24–38.